# Impact of Molecular Packing on Electronic Polarization in Organic Crystals: The Case of Pentacene vs TIPS-Pentacene

Sean M. Ryno, Chad Risko,* and Jean-Luc Brédas*

School of Chemistry and Biochemistry and Center for Organic Photonics and Electronics, Georgia Institute of Technology, Atlanta, Georgia 30332-0400, United States

S *Supporting Information*

ABSTRACT: Polarization energy corresponds to the stabilization of the cation or anion state of an atom or molecule when going from the gas phase to the solid state. The decrease in ionization energy and increase in electron affinity in the solid state are related to the (electronic and nuclear) polarization of the surrounding atoms and molecules in the presence of a charged entity. Here, through a combination of molecular mechanics and quantum mechanics calculations, we evaluate the polarization energies in two prototypical organic semiconductors, pentacene and 6,13-bis(2-(tri-isopropylsilyl)ethynyl)pentacene (TIPS-pentacene). Comparison of the results for the two systems reveals the critical role played by the molecular packing configurations in the determination of the polarization energies and provides physical insight into the experimental data reported by Lichtenberger and co-workers (*J. Amer. Chem. Soc.* **2010**, *132*, 580; *J. Phys. Chem. C* **2010**, *114*, 13838). Our results underline that the impact of packing configurations, well established in the case of the charge-transport properties, also extends to the polarization properties of π-conjugated materials.
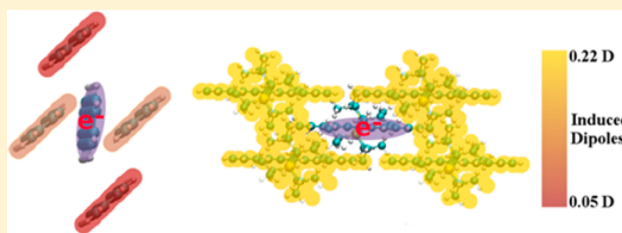
◼ INTRODUCTION

Organic molecular crystals, such as the oligoacenes (i.e., naphthalene, anthracene, tetracene, and pentacene) and their substituted derivatives (e.g., rubrene, alkylsilylethynyl-substituted acenes, or heteroatom-substituted acenes), often serve as representative systems to develop an understanding of the electronic and optical phenomena in π-conjugated electroactive materials.[1−14] Overall, these molecular materials are held together through the interplay among electrostatic (multipole) interactions, dispersion and induction effects, and short-range exchange−repulsion terms.[15−17] A detailed understanding of how these intermolecular interactions determine the available molecular packing arrangements, for both crystalline and disordered materials, is necessary if the full power of computational materials chemistry is to be used to design systems presynthesis, from isolated molecules to bulk packing, and design the materials (e.g., electronic, optical) properties. Increasingly sophisticated methodologies are under development with the goal of predicting molecular packing through a variety of theoretical approaches and are being applied to systems that range from molecular crystals to proteins.[18−22]

Our focus here is on the solid-state electronic polarizations, i.e., the energetic stabilizations of positive [or negative] charges, P_+ [P_-], due to the interactions of the charged entities with their electrostatic environment. The polarization energies can be determined via the Lyons model by examining the change in ionization energy, IE [electron affinity, EA], on going from the gas phase to the solid state.[23] Electronic polarization represents a critical feature in organic electronic materials, as it provides a measure of the energy landscape surrounding charge

carriers,[16,24] which directly impacts the charge-carrier mobilities;[4] it is also expected to play an important role in the charge-separation process in organic solar cells (through charge screening as the electrons and holes move away from the organic−organic interface).[25]

The conjugated backbones of molecular- and polymer-based electronic materials are often appended with linear, branched, and other types of bulky alkyl-based chains to increase solubility and aid in the formulation of inks for solution deposition/printing. However, there is only sparse study of the interplay between electrostatic interactions and molecular packing in bulk solids as a function of the variations in substitution patterns. Recent UPS investigations by Lichtenberger and co-workers[26−28] started to address this issue by comparing the polarization energies of oligoacenes to their tri-isopropylsilylethynyl (TIPS)-substituted counterparts. Interestingly, these studies revealed large variations in the evolution of the IE on going from the gas phase to the solid state as a result of the addition of the TIPS functionality. Lichtenberger and co-workers measured that, in the gas phase, the IEs for pentacene and TIPS-pentacene were 6.54 and 6.28 eV, respectively, indicating that TIPS-pentacene is intrinsically better able to stabilize the resulting positive charge as expected from its more extended conjugation.[28] In thin films, however, pentacene is measured to have a considerably larger polarization energy (1.73 eV; solid-state IE of 4.81 eV) compared to TIPS-pentacene (0.44 eV; solid-state IE of 5.84 eV). Similar trends

are observed for the anthracene- and tetracene-based systems.[26,29,30] Results from Kahn and co-workers[31,32] provide the same qualitative evolutions for TIPS-pentacene and pentacene, although the magnitude of the polarization energies differ; in these studies, the polarization energy of TIPS-pentacene is 1.24 eV (corresponding to an IE of 5.04 eV), while that of pentacene is 0.25 eV larger, 1.49 eV (solid-state IE of 5.05 eV).[31,32]

The quantitative variations found between the Kahn and co-workers data and the Lichtenberger and co-workers data could be related to the differences in the nature of the TIPS-pentacene films used in the photoelectron spectroscopy studies: The measurements from Kahn and co-workers employed a film derived from a polystyrene:TIPS-pentacene blend that is expected to lead to an ordered TIPS-pentacene layer through stratification of TIPS-pentacene at the air interface, while the pristine TIPS-pentacene film grown directly on a polycrystalline gold foil in the work of Lichtenberger and co-workers is suspected to be more disordered.[31,33−35] Hence, these variations, in principle, point to the impact that morphology—which can include deviations in packing configurations and orientations induced by interactions with the substrate or film processing protocol or grain boundaries—can have on the electronic properties of molecular-based materials, which we address in the present work. We note that the large differences in the polarization energies of pentacene and TIPS-pentacene were initially suggested by Lichtenberger and co-workers to be the result of the reduced packing density in TIPS-pentacene (1.104 g/cm^3) compared with (crystalline) pentacene (1.314 g/cm^3).[28]

It is also worth pointing out that the trends concerning the electrochemical oxidation potentials of TIPS-pentacene and pentacene are not clear, as they have been shown to be nearly identical in o-dichlorobenzene[28] but to differ by some 0.3 V in a 0.1 M solution of Bu_4NPF_6 in dichloromethane (with pentacene being more readily oxidized).[36] These discrepancies underline the extreme caution that must be exercised when extrapolating solution electrochemical data to the solid state.[37]

Our goal here is to investigate the impact of the nature of the packing configurations on the polarization energies in the two systems. Pentacene (and the other unsubstituted oligoacenes) packs in a herringbone motif, while TIPS-pentacene displays a well-defined two-dimensional brickwork packing configuration (that can be further altered by the nature of the alkyl groups on the silyl moiety and/or substitution on the acene backbone);[38−40] the packing configurations of TIPS-anthracene and TIPS-tetracene differ from both herringbone and brickwork packings and assume configurations intermediate to those found for pentacene and TIPS-pentacene. Our results demonstrate that the smaller bulk electronic polarization energy of TIPS-pentacene is mainly related to the differences in the nature of the electrostatic interactions, involving the monopole, quadrupole, and induced-dipole moments, that arise from the variations in (explicitly crystalline) packing configurations.[16,41−43]

■ METHODOLOGY

Isolated Molecules. The geometries of the isolated molecules were extracted from the crystal structures. The molecular and crystal structures used throughout the work were taken from the pentacene (PENCEN04),[44] tetracene (TETCEN01),[45] anthracene (ANTCEN09),[46] and TIPS-pentacene (VOQBIM)[38] crystal structures deposited in the Cambridge Structural Database[47,48] (CSD; CSD

identification codes are noted within parentheses), while the crystal structures for TIPS-tetracene and TIPS-anthracene were provided by J. E. Anthony at the University of Kentucky. Quadrupole and electrostatic potential data were calculated at the post Hartree−Fock MP2 level with a 6-31+G(d,p) basis set, as implemented in the Gaussian 09 Revision B.01 program.[49] Polarizability data were obtained with the INDO Hamiltonian using the Mataga-Nishimoto potential to describe Coulomb repulsion via the ZINDO program.[50−52]

Dimer and Cluster Structures. Using the crystal packing configurations, dimers were extracted as neighboring molecules. Total interaction energies and the magnitudes of the noncovalent interactions were determined via symmetry-adapted perturbation theory (SAPT);[15,17,53−59] the Psi4 code was employed for these calculations, with the SAPT(0) truncation used in conjunction with the jun-cc-pvdz basis set.[60] The distributed multipole analysis (DMA) algorithm as implemented in the Molpro program[61] was also used, at the restricted Hartree−Fock level with the 6-311G(d,p) basis set, to evaluate atom-centered multipoles through the 32-pole. The electrostatic interactions were calculated using a custom script based on the derivations of A. J. Stone.[62]

All classical force-field calculations on dimers and larger clusters were carried out with the AMOEBA (Atomic Multipole Optimized Energetics for Biological Applications) force field[63−65] that was parametrized from the results of MP2/6-31+G(d,p) calculations according to a previously reported methodology.[66] The Tinker software suite[67] was used for all force-field calculations. Interaction energies were calculated using the GROUP-INTER and GROUP-MOLECULE keywords to exclude *intra*molecular interactions.

We note that, for the sake of comparison, we also considered brickwork pentacene geometries. These were adapted from TIPS-pentacene structures in which the TIPS groups are removed; the 6 and 13 positions of pentacene are then capped with a hydrogen atom in the position of the *sp*-carbon that was removed.

The polarization energy calculations were carried out using the methodology we recently described,[68] and performed only on molecular packings derived from the crystal structures. Spherical clusters were constructed where molecules with a center-of-mass within a given radius were extracted from a larger supercell. The central molecule is either neutral or takes a negative or positive charge. The polarization energy for a given cluster was calculated using the Lyons model.[16] The bulk polarization energy is determined by increasing the cluster radius and plotting the polarization energy versus the cubic root of the number of molecules in the cluster.

It is important to keep in mind that positively and negatively charged molecules can have different intermolecular interactions with their environments, which leads to an asymmetry in the polarization energies. Thus, P_+ is not necessarily equivalent to P_-. For instance, as we show below, the induced dipole moments resulting from the charges can act to reduce or increase the polarization asymmetry as a function of molecular packing.

■ RESULTS AND DISCUSSION

We first examine the electrostatic properties of the isolated molecules and then turn to dimers to study the intermolecular forces at play and how they change as a function of the molecular packing configurations. Our recently reported approach[68] (that considers large cluster simulations and the AMOEBA polarizable force field) is used to evaluate the bulk electronic polarization; we note that the results from this approach provide a full picture of the anisotropy of polarization effects as opposed to the isotropic polarization derived from continuum models.[29,69,70] All geometries were kept fixed (static geometries); i.e., nuclear polarization is neglected. We focus the majority of the discussion on pentacene and TIPS-pentacene, as similar trends are obtained for the other acenes considered.

Isolated Molecules. The electrostatic potentials (ESPs) reveal that the electron density is distributed in a similar
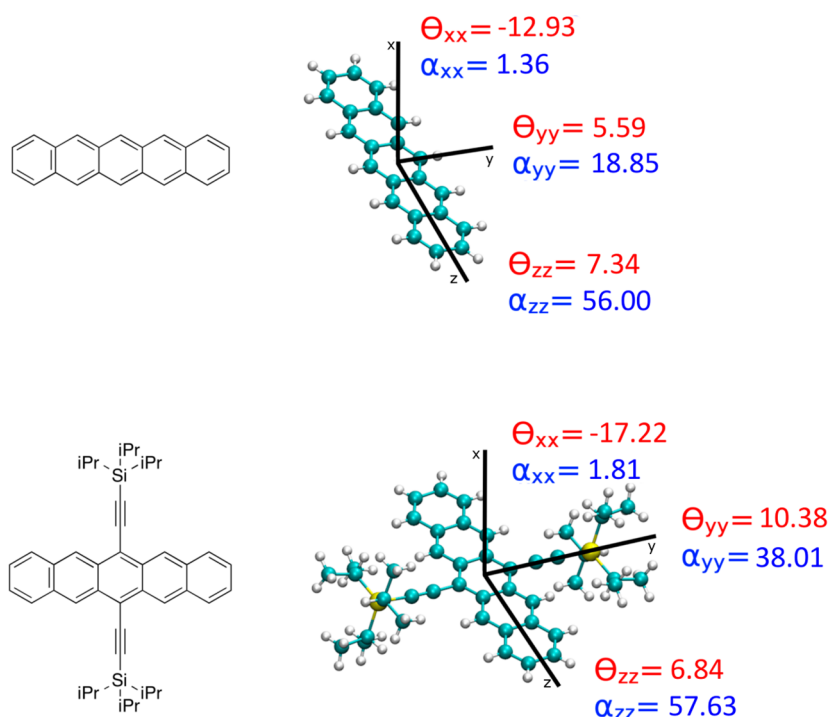
Figure 1. Chemical structures of pentacene (top left) and TIPS-pentacene (bottom left) and ball-and-stick models that display the principal components of the quadrupole (θ in units of Debye-Å) and polarizability (α, in units of Å^3) tensors (center). Quadrupole data were derived from calculations at the MP2/6-31+G(d,p) level, while polarizability data were obtained with the INDO Hamiltonian.[50−52]

Table 1. Dimer Interaction Energies, As Determined by AMOEBA Force-Field Calculations and SAPT(0)/jun-cc-pvdz Calculations, and SAPT(0) Energy Components for Pentacene Herringbone, Pentacene Brickwork, and TIPS-Pentacene[a]

	AMOEBA	SAPT total interaction energy	electrostatic	dispersion	induction	exchange
pentacene herringbone	−10.73	−19.81	−6.51	−26.28	−2.21	15.19
pentacene brickwork	−11.38	−18.14	−6.87	−28.07	−1.83	18.63
TIPS-pentacene	−16.75	−29.16	−8.79	−41.49	−2.13	23.26

[a]All energies in kcal/mol (data for the other dimers are available in the Supporting Information).

manner in both pentacene and TIPS-pentacene and that the attraction/repulsion of a test charge is comparable for both systems (see Supporting Information, SI). As neither pentacene nor TIPS-pentacene possesses a permanent molecular dipole moment, the molecular quadrupole moments dominate the intermolecular electrostatic interactions. In pentacene, a large positive quadrupole component is positioned along the long axis of the backbone (z-axis) with a smaller positive quadrupole component along the backbone short axis (y-axis); a large negative component lies normal to the backbone (x-axis); see Figure 1. These quadrupole components make intuitive sense given that the slightly positively charged hydrogen atoms lie along the periphery of the pentacene backbone plane (defined here as the yz-plane), while the π electron density is perpendicular (x-axis) to the molecular plane. TIPS-pentacene shares a similar positive quadrupole component along the long axis (z-axis), while the presence of TIPS groups makes the y-axis quadrupole component larger as compared to pentacene; again, the component perpendicular to the backbone is large and negative. The linear polarizabilities, likewise, are similar for the two molecules. Hence, based on such modest dissimilarities in the electrostatics and polarizabilities of the isolated molecules, one might not expect a priori the large differences in polarization energy measured for these systems.

Dimer and Cluster Structures. We now turn our attention to pentacene and TIPS-pentacene dimers to obtain insight into the noncovalent interactions at play in the solid state. In particular, we will focus on the interplay among the stabilizing electrostatic, dispersion, and induction interactions and the destabilizing interactions due to electron exchange, through SAPT(0)-based energy decomposition analyses. Of relevance to our comparison between pentacene and TIPS-pentacene are the number of studies on stacked benzene dimers (and derivatives thereof) and the effect of moving from perfectly cofacial (sandwich) configurations to slip-stack and T-shape geometries.[55,57,59,71−75] We note that an important result from these investigations is that simple multipole descriptions of intermolecular interactions do break down for substituted benzene dimers in cofacial configurations at short distances (3.45−3.95 Å).[15] This is related to the increased significance of electrostatic charge penetration, an effect that is not taken into account in current force-field-based methodologies describing solid-state polarization (however, since we are not interested here in optimizing crystal structures but rather use experimentally determined structures, this feature does not alter the conclusions of our classical force-field studies).

To better understand how functionality and packing affect the intermolecular interactions in pentacene and TIPS-pentacene, we have considered three model systems: (i) the

herringbone pentacene dimer, taken from the pentacene crystal structure; (ii) the brickwork TIPS-pentacene dimer, taken from the TIPS-pentacene crystal structure; and (iii) a brickwork pentacene dimer derived from the TIPS-pentacene crystal, with the TIPS functionalities replaced by hydrogen atoms.[76] The SAPT(0) total energies and energy decompositions are reported in Table 1; we recall that noncovalent interaction energies are usually small when compared to chemical bond energies and total (molecular) electronic energies, and as such the differences are expected to be small.[77] From the SAPT(0) interaction energies, the brickwork TIPS-pentacene dimer is found to be more strongly bound with respect to pentacene in the herringbone configuration (∼ −30 kcal/mol vs ∼ −20 kcal/mol). However, a more apples-to-apples comparison is obtained by removing the TIPS moieties and looking at herringbone and brickwork pentacenes. The pentacene brickwork dimer is in fact less stable than the pentacene herringbone dimer by some 1.7 kcal/mol. While the changes to the electrostatic and induction terms essentially offset on going from the herringbone to the brickwork configuration, the increase in the dispersion term in the brickwork configuration is not able to compensate for the additional exchange repulsion that results from the larger overlap of the frontier π-orbitals. The considerable influence of the TIPS-functionality (other than the obvious steric bulk) arises from a large increase in the stabilizing dispersion interactions (by some 13−15 kcal/mol) as compared to either unsubstituted pentacene dimer.

Scaling to the system sizes (up to tens of thousands of atoms) required to study bulk polarization currently relies on the use of classical-based models. Many classical models, though, fail to appropriately describe the intricacies of the intermolecular interactions in sandwich and brickwork structures, often describing the electrostatic interaction as exclusively repulsive.[78] For example, a commonly used methodology for the classical description of electrostatic interactions, the distributed multipole analysis (DMA) method,[79] fails to correctly describe the pentacene structures of interest here: Taking the same series of dimer structures, the DMA results suggest that the pentacene herringbone dimer is the only stable configuration (−1.27 kcal/mol), while the brickwork pentacene (+1.62 kcal/mol) and TIPS-pentacene (+0.95 kcal/mol) dimers are repulsive. While these total interaction energies are clearly incorrect, the individual terms arising from the DMA method (see Tables S3−S7 in the SI) reveal an interesting trend, namely that the quadrupole−quadrupole interactions are stabilizing in herringbone pentacene and destabilizing in the brickwork structures; the quadrupole−quadrupole interactions of these configurations, using the signs of the quadrupole moments derived at the MP2/6-31+G(d,p) level, are depicted qualitatively in Figure 2.

The AMOEBA force field significantly extends beyond simple DMA by not only just including point multipoles (up to quadrupoles) at each atomic site but also incorporating polarization and van der Waals interactions.[65] Hence, the interaction energies derived from the AMOEBA-based analysis of the dimers are all stable (see Table 1) and are about half the values obtained at the SAPT(0) level. The TIPS-pentacene dimer is the most stable in both models; in contrast to SAPT(0), AMOEBA predicts that brickwork pentacene is slightly more stable than the herringbone configuration, a result that arises from stronger van der Waals interactions in the brickwork configuration. Given that the evaluation of the bulk polarization energies mainly deals with longer-range inter-
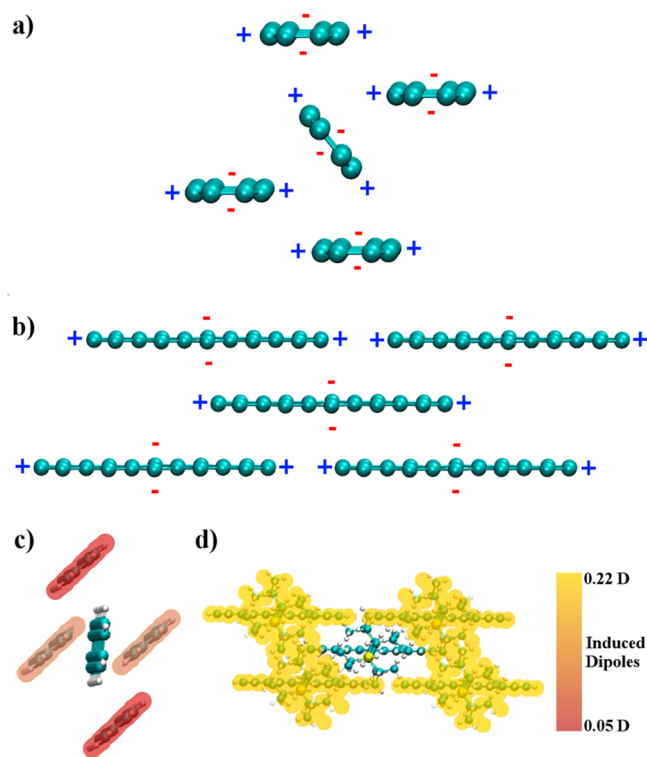

Figure 2. Illustration of the quadrupole interactions in herringbone (a) and brickwork (b) packed pentacene. Parts (c) and (d) display the induced dipoles on the nearest neighbors of a positively charged pentacene and TIPS-pentacene, respectively, determined with the parametrized AMOEBA force field. Dark red molecules in (c) have induced dipoles of 0.059 D, and those in light red have induced dipoles of 0.063 D. All nearest neighbors in (d) have induced dipoles of 0.214 D.

actions (as opposed to the influence of exclusively short-range interactions such as charge penetration) and that we consider only the herringbone pentacene and brickwork TIPS-pentacene configurations whose interaction energies AMOEBA qualitatively describes well, our AMOEBA-based methodology is expected to provide a correct description of the polarization energies.[68]

Figure 2c−d also illustrates the magnitudes of the dipole moments induced by the presence of a positive charge on the central molecule of five-molecule clusters. For pentacene, there is a very slight asymmetry in the induced dipole moments (0.063 D vs 0.059 D) in the herringbone packing configuration. Importantly, the induced dipole moments are much larger in TIPS-pentacene (0.21 D for all neighbors, with no asymmetry observed). These differences point to another key dissimilarity as a function of molecular packing and indicate that induced dipole moments will be of considerable importance in the stabilization of charge carriers in the brickwork-packed TIPS-pentacene.

In view of the above discussion, it can be anticipated that quadrupole and induced-dipole effects will strongly impact the bulk electronic polarizations. Charge-permanent-quadrupole interactions in the systems here (we recall that these molecules possess no permanent dipole moment) are expected to have considerable contribution to the magnitude and asymmetry (due to differences in the sign of the charge) of the electronic polarization; on the other hand, the induced-dipole interactions are expected to act to reduce the asymmetry so as to stabilize

the charge and, depending on the local quadrupoles, will result in varying degrees of stabilization.

Bulk-like Systems. We now expand the system sizes under consideration through a range of clusters that can include upward of many thousands of atoms by relying on our recently described approach to evaluate the bulk electronic polarizations.[68] The results presented in Figure 3 show that the bulk
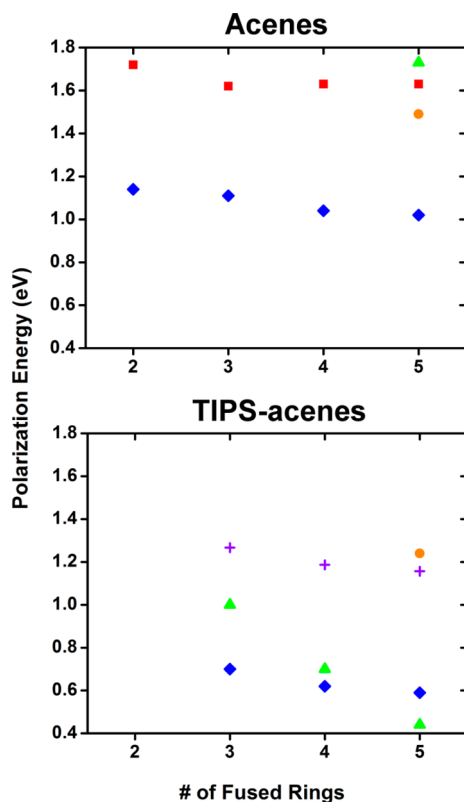

Figure 3. Bulk polarization energies due to a hole for oligoacenes (top) and TIPS-substituted acenes (bottom) as calculated here (◆) or reported from experimental measurements by Sato et al.[29] (■), Griffith et al.[26] (▲), and Qi et al.[31] (●). We also show (+) the calculated values for the TIPS-substituted acenes corrected by the average difference between the calculated and experimental values for the oligoacenes.

polarization energy for positive charges (holes) is some 0.4 eV larger in pentacene (1.02 eV) than in TIPS-pentacene (0.59 eV), which is in good general agreement with the experimental results reported by Kahn and co-workers.[26−28,31] The polarization energies for negative charges (electrons) are 0.79 eV in pentacene (∼0.2 eV *smaller* than that for holes) and 0.69 eV in TIPS-pentacene (∼0.1 eV *larger* than that for holes). In pentacene, experimental data confirm that the electronic polarization energy for a hole is larger than that for an electron; the same holds true for the other unsubstituted acenes.[29,30,80,81]

That there is a difference as to which charge carrier leads to the larger polarization energy in TIPS-pentacene vs pentacene is an interesting consequence of the molecular packing configurations. If we first examine the contributions to the polarization energy arising solely from the permanent multipole moments (i.e., monopole–quadrupole and quadrupole–quadrupole interactions), we obtain that (i) TIPS-pentacene has a larger polarization energy asymmetry than pentacene (0.67 eV vs 0.45 eV for the largest clusters, respectively) and (ii) both

systems have larger polarization energies for holes than for electrons. This picture changes dramatically when the induced dipoles are included: (i) the polarization energy asymmetries markedly decrease, with that for TIPS-pentacene (0.10 eV) now being smaller than that for pentacene (0.23 eV); and (ii) the electron in TIPS-pentacene becomes the charge carrier with the larger polarization energy. Hence, the interplay between the molecular packing structures and the permanent multipole and induced-dipole moments plays a defining role in determining the polarization in these materials.

We now turn to a discussion of the polarization energy for holes as a function of oligoacene length (see Figures S2−S4 in the SI). There occurs a modest decrease in polarization energy for the unsubstituted oligoacenes as the molecular backbone expands, with the calculated evolution (0.12 eV decrease from 1.14 eV for naphthalene to 1.02 eV for pentacene)[66] being in excellent agreement with the experimental data of Sato et al. (0.09 eV decrease from 1.72 eV for naphthalene to 1.63 eV for pentacene).[28] (The differences between theory and experiment in terms of the absolute values of the P_+ energies were discussed in ref 68.) Overall, the decrease of P_+ as a function of increased acene length can be related to the expanded distribution of the hole across the molecule that reduces the size of the charge−quadrupole interactions.[82]

For the TIPS-acenes, we calculate a similar decrease (0.11 eV from 0.70 eV for TIPS-anthracene to 0.59 eV for TIPS-pentacene). The evolution measured by Lichtenberger and co-workers in the TIPS-substituted acenes is quantitatively much larger: P_+ for TIPS-anthracene (1.00 eV) is measured by these authors to be some 0.5 eV larger than P_+ for TIPS-pentacene (0.44 eV).[26,28] However, our calculated difference between the P_+ energies of pentacene and TIPS-pentacene, 0.43 eV, is much closer to the value measured by Kahn and co-workers, 0.25 eV, than that measured by Lichtenberger and co-workers, 1.29 eV. In fact, if we correct the calculated value of P_+ for TIPS-pentacene by the average difference in calculated vs experimental P_+ values for the oligoacenes, we obtain an estimated value for the TIPS-pentacene P_+ within 0.1 eV of the P_+ value measured by Kahn and co-workers; see bottom of Figure 3. The better agreement between our results based on the crystal structure of TIPS-pentacene and the data from Kahn and co-workers measured on ordered thin films vs the data from Lichtenberger and co-workers obtained on more disordered films *underlines the importance of morphology and local packing configurations in determining polarization energies.*

■ CONCLUSION

We have presented a combined quantum mechanics/molecular mechanics description of the polarization energies for holes and electrons in the unsubstituted and TIPS-substituted acene series. Through a multiscale theoretical approach, we have developed a picture founded in basic electrostatics that explains the origin of the markedly different polarization energies in the two types of systems. Use of a polarizable force field that includes quadrupole and induced-dipole interactions has allowed us to depict how electrostatic interactions change on going from the (oligoacene) herringbone motif to the (TIPS-substituted acene) brickwork packing structure. Though these systems show very similar electronic and electrostatic characteristics for the isolated molecules, the variations in solid-state packing induce very different electronic polarization effects; e.g., the Coulombically favorable intermolecular quadrupole interactions in the pentacene herringbone motif are not accessible to

TIPS-pentacene due to variations in molecular packing caused by the presence of the bulky TIPS groups.

These results help clarify previous experimental findings[26−28] by providing an in-depth picture of the electrostatic interactions that result in the shift of the ionization energies on going from the gas phase to the solid state, and offer general insight into the bulk polarization energy in these materials. The brickwork configuration of TIPS-pentacene leads to a fundamental change in the quadrupole and induced-dipole interactions, resulting in smaller bulk polarization energy compared to pentacene.

The main message of our work is that *the impact of molecular packing configurations*, well established in the case of the charge-carrier transport and optical properties,[26−28,68,83−86] also *extends to the polarization properties of π-conjugated materials*. The work also underlines that extreme care has to be taken when extrapolating solution electrochemical data (a long time-scale thermodynamic equilibrium measure that includes entropy) for oxidation and reduction potentials to solid-state ionization energies and electron affinities (spectroscopic-based, short-time scale measurements).

■ ASSOCIATED CONTENT

Ⓢ Supporting Information

A table of dimer interaction energies including DMA electrostatic interaction energies through 32-pole, extrapolated polarization energies, additional SAPT results, ESP plots, and structures used in this paper are available in the Supporting Information. This material is available free of charge via the Internet at http://pubs.acs.org.

■ AUTHOR INFORMATION

Corresponding Authors
chad.risko@chemistry.gatech.edu
jean-luc.bredas@chemistry.gatech.edu

Notes
The authors declare no competing financial interest.

■ ACKNOWLEDGMENTS

■ REFERENCES

(1) Zschieschang, U.; Kang, M. J.; Takimiya, K.; Sekitani, T.; Someya, T.; Canzler, T. W.; Werner, A.; Blochwitz-Nimoth, J.; Klauk, H. *J. Mater. Chem.* **2012**, *22*, 4273.

(2) Ou-Yang, W.; Uemura, T.; Miyake, K.; Onish, S.; Kato, T.; Katayama, M.; Kang, M.; Takimiya, K.; Ikeda, M.; Kuwabara, H.; Hamada, M.; Takeya, J. *Appl. Phys. Lett.* **2012**, *101*, 223304.

(3) Valeev, E. F.; Coropceanu, V.; Filho, D. A. d. S.; Salman, S.; Bredas, J. L. *J. Am. Chem. Soc.* **2006**, *128*, 9882.

(4) Coropceanu, V.; Cornil, J.; Silva, D. A. d.; Olivier, Y.; Silbey, R.; Bredas, J. L. *Chem. Rev.* **2007**, *107*, 926.

(5) Bakulin, A. A.; Rao, A.; Pavelyev, V. G.; van Loosdrecht, P. H. M.; Pshenichnikov, M. S.; Niedzialek, D.; Cornil, J.; Beljonne, D.; Friend, R. H. *Science* **2012**, *335*, 1340.

(6) Ahn, T.-S.; Muller, A. M.; Al-Kaysi, R. O.; Spano, F. C.; Norton, J. E.; Beljonne, D.; Bredas, J.-L.; Bardeen, C. J. *J. Chem. Phys.* **2008**, *128*, 054505.

(7) Saigusa, H.; Lim, E. C. *J. Phys. Chem.* **1994**, *98*, 13470.

(8) Sai, N.; Barbara, P. F.; Leung, K. *Phys. Rev. Lett.* **2011**, *106*, 226403.

(9) van Dijk, L.; Spano, F. C.; Bobbert, P. A. *Chem. Phys. Lett.* **2012**, *529*, 69.

(10) Müller, A. M.; Avlasevich, Y. S.; Schoeller, W. W.; Müllen, K.; Bardeen, C. J. *J. Am. Chem. Soc.* **2007**, *129*, 14240.

(11) Wilson, M. W. B.; Rao, A.; Clark, J.; Kumar, R. S. S.; Brida, D.; Cerullo, G.; Friend, R. H. *J. Am. Chem. Soc.* **2011**, *133*, 11830.

(12) Jadhav, P. J.; Brown, P. R.; Thompson, N.; Wunsch, B.; Mohanty, A.; Yost, S. R.; Hontz, E.; Van Voorhis, T.; Bawendi, M. G.; Bulović, V.; Baldo, M. A. *Adv. Mater.* **2012**, *24*, 6169.

(13) Roberts, S. T.; McAnally, R. E.; Mastron, J. N.; Webber, D. H.; Whited, M. T.; Brutchey, R. L.; Thompson, M. E.; Bradforth, S. E. *J. Am. Chem. Soc.* **2012**, *134*, 6388.

(14) Smith, M. B.; Michl, J. *Chem. Rev.* **2010**, *110*, 6891.

(15) Hohenstein, E. G.; Duan, J.; Sherrill, C. D. *J. Am. Chem. Soc.* **2011**, *133*, 13244.

(16) Silinsh, E. A. *Organic Molecular Crystals: Their Electronic States*; Springer: New York, 1980.

(17) Sherrill, C. D. *Acc. Chem. Res.* **2013**, *46*, 1020.

(18) Neumann, M. A.; Leusen, F. J. J.; Kendrick, J. *Angew. Chem., Int. Ed.* **2008**, *47*, 2427.

(19) Neumann, M. A. *J. Phys. Chem. B* **2008**, *112*, 9810.

(20) Sanderson, K. *Nature* **2007**, *450*, 771.

(21) Price, S. L.; Leslie, M.; Welch, G. W. A.; Habgood, M.; Price, L. S.; Karamertzanis, P. G.; Day, G. M. *Phys. Chem. Chem. Phys.* **2010**, *12*, 8478.

(22) Zhou, H.; Skolnick, J. *Biophys. J.* **2011**, *101*, 2043.

(23) Gutmann, F.; Lyons, L. E. *Organic Semiconductors*; Wiley: New York, 1967.

(24) Silinsh, E. A.; Capek, V. *Organic Molecular Crystals: Interaction, Localization, and Transport Phenomena*; AIP: New York, 1994.

(25) Bredas, J. L.; Norton, J. E.; Cornil, J.; Coropceanu, V. *Acc. Chem. Res.* **2009**, *42*, 1691.

(26) Griffith, O. L.; Jones, A. G.; Anthony, J. E.; Lichtenberger, D. L. *J. Phys. Chem. C* **2010**, *114*, 13838.

(27) Griffith, O. L.; Anthony, J. E.; Jones, A. G.; Shu, Y.; Lichtenberger, D. L. *J. Am. Chem. Soc.* **2012**, *134*, 14185.

(28) Griffith, O. L.; Anthony, J. E.; Jones, A. G.; Lichtenberger, D. L. *J. Am. Chem. Soc.* **2010**, *132*, 580.

(29) Sato, N.; Inokuchi, H.; Silinsh, E. A. *Chem. Phys.* **1987**, *115*, 269.

(30) Pope, M.; Burgos, J.; Giachino, J. *J. Chem. Phys.* **1965**, *43*, 3367.

(31) Qi, Y.; Mohapatra, S. K.; Kim, S. B.; Barlow, S.; Marder, S. R.; Kahn, A. *Appl. Phys. Lett.* **2012**, *100*, 083305.

(32) Chan, C.; Kahn, A. *Appl. Phys. A: Mater. Sci. Process.* **2009**, *95*, 7.

(33) Madec, M. B.; Crouch, D.; Llorente, G. R.; Whittle, T. J.; Geoghegan, M.; Yeates, S. G. *J. Mater. Chem.* **2008**, *18*, 3230.

(34) Smith, J.; Hamilton, R.; McCulloch, I.; Stingelin-Stutzmann, N.; Henney, M.; Bradley, D. D. C.; Anthopoulos, T. D. *J. Mater. Chem.* **2010**, *20*, 2562.

(35) Hwang, D. Y.; Fuentes-Hernandez, C.; Berrigan, J. D.; Fang, Y.; Kim, J.; W. J. Potscavage, J.; Cheun, H.; Sandhage, K. H.; Kippelen, B. *J. Mater. Chem.* **2012**, *22*, 5531.

(36) Anthony, J. E.; Swartz, C. R.; Landis, C. A.; Parkin, S. R. *Proceedings of SPIE* **2005**, *5940*, 594002.

(37) Bredas, J.-L. *Materials Horizons* **2014**, *1*, 17.

(38) Brooks, J. S.; Eaton, D. L.; Parkin, S. R.; Anthony, J. E. *J. Am. Chem. Soc.* **2001**, *123*, 9482.

(39) Chen, J.; Subramanian, S.; Parkin, S. R.; Siegler, M.; Gallup, K.; Haughn, C.; Martin, D. C.; Anthony, J. E. *J. Mater. Chem.* **2008**, *18*, 1961.

(40) Chen, J.; Anthony, J.; Martin, D. C. *J. Phys. Chem. B* **2006**, *110*, 16397.

(41) Campbell, R. B.; Robertson, J. M.; Trotter, J. *Acta Crystallogr.* **1961**, *14*, 705.

(42) Anthony, J. E. *Angew. Chem., Int. Ed.* **2008**, *47*, 452.

(43) Lyons, L. E. *J. Chem. Soc.* **1957**, 5001.

(44) Mattheus, C. C.; Dros, A. B.; Baas, J.; Meetsma, A.; Boer, J. L. d.; Palstra, T. T. M. *Acta Crystallogr., Sect. C: Cryst. Struct. Commun.* **2001**, *57*, 939.

(45) Holmes, D.; Kumaraswamy, S.; Matzger, A. J.; Vollhardt, K. P. C. *Chem.—Eur. J.* **1999**, *5*, 3399.

(46) Brock, C. P.; Dunitz, J. D. *Acta Crystallogr., Sect. B* **1990**, *B46*, 795.

(47) Allen, F. H. *Acta Crystallogr.* **2002**, *B58*, 380.

(48) Fletcher, D. A.; McMeeking, R. F.; Parkin, D. *J. Chem. Inf. Comput. Sci.* **1996**, *36*, 746.

(49) Frisch, M. J.; Trucks, G. W.; Schlegel, H. B.; Scuseria, G. E.; Robb, M. A.; Cheeseman, J. R.; Scalmani, G.; Barone, V.; Mennucci, B.; Petersson, G. A.; Nakatsuji, H.; Caricato, M.; Li, X.; Hratchian, H. P.; Izmaylov, A. F.; Bloino, J.; Zheng, G.; Sonnenberg, J. L.; Hada, M.; Ehara, M.; Toyota, K.; Fukuda, R.; Hasegawa, J.; Ishida, M.; Nakajima, T.; Honda, Y.; Kitao, O.; Nakai, H.; Vreven, T.; Montgomery, J. A.; Peralta, J. E.; Ogliaro, F.; Bearpark, M.; Heyd, J. J.; Brothers, E.; Kudin, K. N.; Staroverov, V. N.; Kobayashi, R.; Normand, J.; Raghavachari, K.; Rendell, A.; Burant, J. C.; Iyengar, S. S.; Tomasi, J.; Cossi, M.; Rega, N.; Millam, J. M.; Klene, M.; Knox, J. E.; Cross, J. B.; Bakken, V.; Adamo, C.; Jaramillo, J.; Gomperts, R.; Stratmann, R. E.; Yazyev, O.; Austin, A. J.; Cammi, R.; Pomelli, C.; Ochterski, J. W.; Martin, R. L.; Morokuma, K.; Zakrzewski, V. G.; Voth, G. A.; Salvador, P.; Dannenberg, J. J.; Dapprich, S.; Daniels, A. D.; Farkas; Foresman, J. B.; Ortiz, J. V.; Cioslowski, J.; Fox, D. J. *Gaussian 09*, Revision B.01; Gaussian, Inc.: Wallingford, CT, 2009.

(50) Ridley, J.; Zerner, M. *Theor. Chim. Acta* **1973**, *32*, 111.

(51) Nishimoto, K.; Mataga, N. *Z. Phys. Chem. (Muenchen, Ger.)* **1957**, *12*, 335.

(52) Mataga, N.; Nishimoto, K. *Z. Phys. Chem. (Muenchen, Ger.)* **1957**, *13*, 140.

(53) Jeziorski, B.; Moszynski, R.; Szalewicz, K. *Chem. Rev.* **1994**, *94*, 1887.

(54) Sinnokrot, M. O.; Sherrill, C. D. *J. Am. Chem. Soc.* **2004**, *126*, 7690.

(55) Sinnokrot, M. O.; Sherrill, C. D. *J. Phys. Chem. A* **2006**, *110*, 10656.

(56) Arnstein, S. A.; Sherrill, C. D. *Phys. Chem. Chem. Phys.* **2008**, *10*, 2646.

(57) Ringer, A. L.; Sherrill, C. D. *J. Am. Chem. Soc.* **2009**, *131*, 4574.

(58) Geng, Y.; Takatani, T.; Hohenstein, E. G.; Sherrill, C. D. *J. Phys. Chem. A* **2010**, *114*, 3576.

(59) Hohenstein, E. G.; Sherrill, C. D. *J. Chem. Phys.* **2010**, *132*, 184111.

(60) Turney, J. M.; Simmonett, A. C.; Parrish, R. M.; Hohenstein, E. G.; Evangelista, F. A.; Fermann, J. T.; Mintz, B. J.; Burns, L. A.; Wilke, J. J.; Abrams, M. L.; Russ, N. J.; Leininger, M. L.; Janssen, C. L.; Seidl, E. T.; Allen, W. D.; Schaefer, H. F.; King, R. A.; Valeev, E. F.; Sherrill, C. D.; Crawford, T. D. *Wiley Interdisciplinary Reviews: Computational Molecular Science* **2012**, *2*, 556.

(61) Werner, H.-J.; Knowles, P. J.; Knizia, G.; Manby, F. R.; Schütz, M.; Celani, P.; Korona, T.; Lindh, R.; Mitrushenkov, A.; Rauhut, G.; Shamasundar, K. R.; Adler, T. B.; Amos, R. D.; Bernhardsson, A.; Berning, A.; Cooper, D. L.; Deegan, M. J. O.; Dobbyn, A. J.; Eckert, F.; Goll, E.; Hampel, C.; Hesselmann, A.; Hetzer, G.; Hrenar, T.; Jansen, G.; Köppl, C.; Liu, Y.; Lloyd, A. W.; Mata, R. A.; May, A. J.; McNicholas, S. J.; Meyer, W.; Mura, M. E.; Nicklass, A.; O'Neill, D. P.; Palmieri, P.; Peng, D.; Pflüger, K.; Pitzer, R.; Reiher, M.; Shiozaki, T.; Stoll, H.; Stone, A. J.; Tarroni, R.; Thorsteinsson, T.; Wang, M. *Molpro*; Cardiff, U.K., 2012.

(62) Stone, A. J. *The Theory of Intermolecular Forces*; Clarendon Press: Oxford, 1996.

(63) Ren, P.; Ponder, J. W. *J. Comput. Chem.* **2002**, *23*, 1497.

(64) Ren, P.; Ponder, J. W. *J. Phys. Chem. B* **2003**, *107*, 5933.

(65) Ponder, J. W.; Wu, C.; Ren, P.; Pande, V. S.; Chodera, J. D.; Schnieders, M. J.; Haque, I.; Mobley, D. L.; Lambrecht, D. S.; DiStasio, R. A.; Head-Gordon, M.; Clark, G. N. I.; Johnson, M. E.; Head-Gordon, T. *J. Phys. Chem. B* **2010**, *114*, 2549.

(66) Head-Gordon, M.; Pople, J. A.; Frisch, M. J. *Chem. Phys. Lett.* **1988**, *153*, 503.

(67) Ponder, J. W. *Tinker: Software Tools for Molecular Design*, 6.0, 2012.

(68) Ryno, S. M.; Lee, S. R.; Sears, J.; Risko, C.; Bredas, J. L. *J. Phys. Chem. C* **2013**, *117*, 13853.

(69) Sato, N.; Seki, K.; Inokuchi, H. *J. Chem. Soc., Faraday Trans. 2* **1981**, *77*, 1621.

(70) Sato, N.; Saito, G.; Inokuchi, H. *Chem. Phys.* **1983**, *76*, 79.

(71) Jaeger, H. M.; Schaefer, H. F.; Hohenstein, E. G.; David Sherrill, C. *Computational and Theoretical Chemistry* **2011**, *973*, 47.

(72) Seo, J.-I.; Kim, I.; Lee, Y. S. *Chem. Phys. Lett.* **2009**, *474*, 101.

(73) Lutz, P. B.; Bayse, C. A. *Phys. Chem. Chem. Phys.* **2013**, *15*, 9397.

(74) Ansorg, K.; Tafipolsky, M.; Engels, B. *J. Phys. Chem. B* **2013**, *117*, 10093.

(75) Podeszwa, R.; Bukowski, R.; Szalewicz, K. *J. Phys. Chem. A* **2006**, *110*, 10345.

(76) It is important to note that previous studies have used idealized structures for consideration of the nonbonded interactions. The systems that are of interest here, being experimentally determined, are not idealized from both a rotational and displacement perspective. For example, the herringbone pentacene is not perfectly T-shaped having an offset angle of 52° from ideal.

(77) Szalewicz, K. *Wiley Interdisciplinary Reviews: Computational Molecular Science* **2012**, *2*, 254.

(78) Sherrill, C. D.; Takatani, T.; Hohenstein, E. G. *J. Phys. Chem. A* **2009**, *113*, 10146.

(79) Stone, A. J. *Chem. Phys. Lett.* **1981**, *83*, 233.

(80) Ando, N.; Mitsui, M.; Nakajima, A. *J. Chem. Phys.* **2008**, *128*, 154318.

(81) Berry, R. S.; Jortner, J.; Mackie, J. C.; Pysh, E. S.; Rice, S. A. *J. Chem. Phys.* **1965**, *42*, 1535.

(82) As the acene length increases, the charge carrier (hole or electron) becomes more distributed along the molecule. This results in a decrease of the magnitude of the atomic charge at each atom site. In addition, the molecular quadrupole moments increase with acene length, with the atomic-centered quadrupole moments maintaining a consistent value across the series. The combination of these effects leads to overall smaller monopole−quadrupole interactions as a function of increased acene length.

(83) Beaujuge, P. M.; Tsao, H. N.; Hansen, M. R.; Amb, C. M.; Risko, C.; Subbiah, J.; Choudhury, K. R.; Mavrinskiy, A.; Pisula, W.; Brédas, J.-L.; So, F.; Müllen, K.; Reynolds, J. R. *J. Am. Chem. Soc.* **2012**, *134*, 8944.

(84) Pingel, P.; Zen, A.; Abellón, R. D.; Grozema, F. C.; Siebbeles, L. D. A.; Neher, D. *Adv. Funct. Mater.* **2010**, *20*, 2286.

(85) Noriega, R.; Rivnay, J.; Vandewal, K.; Koch, F. P. V.; Stingelin, N.; Smith, P.; Toney, M. F.; Salleo, A. *Nat. Mater.* **2013**, *12*, 1038.

(86) Clark, J.; Silva, C.; Friend, R. H.; Spano, F. C. *Phys. Rev. Lett.* **2007**, *98*, 206406.